

Electron localisation and interaction effects in three-dimensional Au-Si amorphous alloys and Au/Si multilayers

This article has been downloaded from IOPscience. Please scroll down to see the full text article.

1990 J. Phys.: Condens. Matter 2 377

(<http://iopscience.iop.org/0953-8984/2/2/013>)

View [the table of contents for this issue](#), or go to the [journal homepage](#) for more

Download details:

IP Address: 171.66.16.96

The article was downloaded on 10/05/2010 at 21:26

Please note that [terms and conditions apply](#).

Electron localisation and interaction effects in three-dimensional Au–Si amorphous alloys and Au/Si multilayers

A Audouard^{†‡}, N Cherradi[†], J M Broto^{‡§}, G Marchal[†] and A Fert[§]

[†] Laboratoire de Physique du Solide, Université de Nancy I, BP 239, 54506 Vandoeuvre Les Nancy, France

[‡] Laboratoire de Physique des Solides et Service des Champs Magnétiques Intenses, Institut National des Sciences Appliquées, Université Paul Sabatier, Avenue de Rangueil, 31077 Toulouse, France

[§] Laboratoire de Physique des Solides, Université de Paris-Sud, 91405 Orsay, France

Received 30 June 1989

Abstract. We have studied the temperature and magnetic field dependence of the conductivity of $\text{Au}_x\text{Si}_{1-x}$ amorphous alloys ($0.17 \leq x \leq 0.73$) and Au/Si multilayers with individual layer thickness t_{Si} from 14 Å to 16 Å and t_{Au} from 5 Å to 16 Å. The three-dimensional electron localisation and interaction models correctly account for the data of both types of samples. Analysis of magnetoresistance and conductivity data yields consistent results which allow us to derive the temperature dependence of the inelastic scattering rate: close results are obtained both for amorphous alloys and multilayers.

1. Introduction

It is now well established that electron localisation and interaction phenomena dominate the electron transport properties of disordered metallic systems. In particular, the temperature and magnetic field dependence of the conductivity of two-dimensional (2D) thin metal films (Bergmann 1984) and three-dimensional (3D) amorphous alloys (Howson and Gallagher 1988) are both correctly described by the theory.

Electron transport properties of heterogeneous systems, especially those of semi-conducting granular metal films, have been studied for many years (Abeles *et al* 1975). It is, however, only very recently that electron localisation and interaction phenomena become considered in metallic granular films: Carl *et al* (1989) reported on the 2D electron transport properties of $\text{Pt}_x\text{C}_{1-x}$ system which were well accounted for by the theory. The problem that arises is then to understand the influence of the microstructure on the low temperature electron transport properties and to decide whether or not electron localisation and interaction phenomena take place in a 3D heterogeneous system.

In order to gain further insight into this problem, we have studied the electron transport properties of the heterogeneous Au–Si system. Two types of samples were considered: (i) amorphous $\text{Au}_x\text{Si}_{1-x}$ alloys and (ii) Au/Si multilayers with thin individual layer thicknesses.

$\text{Au}_x\text{Si}_{1-x}$ alloys can be obtained amorphous in the concentration range $0 \leq x \leq 0.8$ when prepared by co-evaporation of Au and Si. Electron diffraction studies (Mangin *et al* 1980) have shown that amorphous $\text{Au}_x\text{Si}_{1-x}$ thin films are two-phased and composed of a mixture of respectively Au-rich and Si-rich phases. A direct confirmation of the coexistence of the two phases was obtained by scanning transmission and high resolution electron diffraction on an amorphous $\text{Au}_{0.17}\text{Si}_{0.83}$ thin film (Audier *et al* 1985). These results are in agreement with the reported data on both the conductivity behaviour of semiconducting alloys ($x \leq 0.13$) (Audouard *et al* 1989) and on the superconducting properties of metallic alloys ($0.22 \leq x \leq 0.76$) (Cherradi *et al* 1989a) which suggested that Si-rich and Au-rich phases have gold concentrations $x \approx 0.09$ and $x \approx 0.75$ respectively.

The electron transport properties of Au/Si multilayers strongly depend on the silicon layer thickness. For $t_{\text{Si}} \geq 30 \text{ \AA}$, the conductivity exhibits a two-dimensional behaviour (Cherradi *et al* 1989b) whereas, when t_{Si} is about 15 \AA , a 3D conductivity is observed: such multilayers exhibit superconductivity as alloys do (Cherradi *et al* 1989a). This behaviour as a function of t_{Si} is certainly due to intermixing between gold and silicon layers. Indeed, in most of metal/Si multilayers, intermixing leads to the formation of amorphous interfaces of about 15 to 20 \AA in thickness (Brasen *et al* 1986, Petford-Long *et al* 1987, Dufour *et al* 1989). In the case of Au/Si multilayers, metallic layers are amorphous when t_{Au} is lower than about 20 \AA (Cherradi *et al* 1989a, b) which suggests intermixing over this length scale in the Au/Si system. It was however verified by cross-sectional transmission electron microscopy experiments that a compositional modulation is still present across the film, even for very thin Si layers. Those multilayers can then be regarded (alike amorphous alloys but with a different morphology) as composed of alternatively Au-rich and Si-rich amorphous regions.

In this paper we report on the temperature and magnetic field dependence of the conductivity of the both kinds of samples. The analysis of the experimental data in the framework of the 3D electron localisation and interaction theories lead to consistent results which allows the determination of the inelastic scattering rate in each case. It is shown that, at a given mean composition, both alloys and multilayers exhibit the same behaviour.

2. Experimental procedure

$\text{Au}_x\text{Si}_{1-x}$ alloys and Au/Si multilayers were prepared in ultra high vacuum ($P \leq 3 \times 10^{-8}$ torr during evaporation) by condensation of gold and silicon onto substrates held at liquid nitrogen temperature. Gold was melted in a tungsten crucible while silicon was evaporated with an electron gun. The evaporation rates of both elements were monitored using quartz balances system. Resistance samples were condensed onto Corning 7059 glass plates with previously evaporated gold electrodes. $\text{Au}_x\text{Si}_{1-x}$ amorphous films with x ranging from 0.17 to 0.73 and total thickness about 500 \AA were obtained by simultaneous condensation of both elements. Au/Si multilayers were obtained by depositing alternatively 20 layers of silicon and gold covered with an extra silicon layer. The individual gold layers thickness t_{Au} were between 5 \AA and 16 \AA , whereas the individual silicon layer thicknesses t_{Si} were between 14 \AA and 16 \AA . Electrical resistance and magnetoresistance measurements were performed using the conventional four-probe method on samples heated up to room temperature after evaporation. The experiments were carried out in He-bath cryostats, equipped with a superconducting coil ($H = 7 \text{ T}$) for the magnetoresistance experiments.

Table 1. Data on the samples submitted to magnetoresistance experiments. T_c is the superconducting transition temperature and x is the mean Au concentration in the multilayers.

Sample composition	T_c (K)
a-Au _{0.17} Si _{0.83}	<0.01
a-Au _{0.20} Si _{0.80}	<0.01
a-Au _{0.25} Si _{0.75}	0.14
a-Au _{0.35} Si _{0.65}	0.72
a-Au _{0.53} Si _{0.47}	1.25
Multilayers	•
Au(6.5 Å)/Si(16 Å), $x = 0.34$	0.42
Au(9 Å)/Si(16 Å), $x = 0.42$	0.60

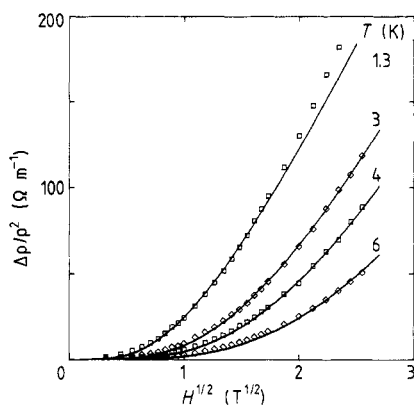


Figure 1. Magnetoresistance of the amorphous alloy Au_{0.17}Si_{0.83} at different temperatures. Full curves are best fits to experimental data (see text).

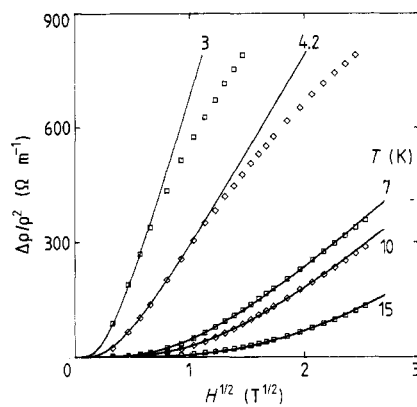


Figure 2. As in figure 1 except for amorphous alloy Au_{0.35}Si_{0.65}.

3. Results and discussion

3.1. Magnetoresistance

Magnetoresistance data were recorded on five amorphous alloys and two multilayers (cf table 1). Three examples are shown on figures 1 to 3, it can be remarked that close behaviour is observed for alloys and multilayers of same mean composition (cf figures 2 and 3). It was moreover verified that the magnetoresistance anisotropy is very weak for both kinds of samples, in particular that of multilayers. These results suggest a 3D behaviour for multilayers with thin Si layers as already reported (Cherradi *et al* 1989a, b).

In the absence of magnetic scattering, the magnetoresistance arising from 3D localisation effects is expressed as (Al'tshuler *et al* 1981)

$$\Delta\rho/\rho^2 = \alpha_H(e^2/2\pi^2\hbar)(eH/\hbar)^{1/2}[(\frac{1}{2} + \beta)f_3(H/H_i) - 3/2f_3(H/H_1)] \quad (1)$$

in which f_3 is the function given by Kawabata (1980), α_H equals 1 in a free electron

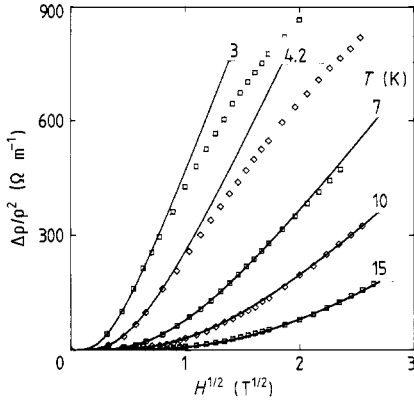


Figure 3. As in figure 1 except for the multilayer Au(6.5 Å)/Si(16 Å).

model, β is a parameter which takes into account the superconducting fluctuations (Larkin 1980) and H_1 is defined as $H_1 = H_i + 2H_{so}$ with

$$H_1 \tau_i = H_{so} \tau_{so} = \hbar/4eD \quad (2)$$

where τ_i and τ_{so} are the mean electron scattering time for inelastic and spin-orbit scattering respectively and D is the diffusion constant. The contribution of electron-electron interaction (spin splitting) was calculated by Lee and Ramakrishnan (1982) as

$$\Delta\rho/\rho^2 = \alpha_H (e^2/4\pi^2\hbar) F_\sigma (kT/2D\hbar)^{1/2} g_3 (g\mu_B H/kT) \quad (3)$$

where (Lee and Ramakrishnan 1985)

$$F_\sigma = \frac{32}{3} F [(1 + \frac{1}{2}F)^{3/2} - 1 - \frac{3}{4}F]. \quad (4)$$

In the following, the functions f_3 and g_3 are calculated using the analytical form given by Ousset *et al* (1985). The diffusion constant D and the screening factor F are calculated according to a free electron model assuming homogeneous alloys, as previously done in the case of 2D granular Pt-C films by Carl *et al* (1989). It is worth noting that the contribution of electron-electron interaction (particle-particle channel) is negligible in the gold concentration range $0.17 \leq x \leq 0.53$ and that the contribution of electron-electron interaction (spin-splitting) is negligible as soon as the gold concentration reaches $x = 0.25$. A positive magnetoresistance with no maximum as a function of the magnetic field up to 6.5 Tesla is evidenced on figures 1 to 3. This behaviour is the signature of the strong spin-orbit coupling induced by gold atoms which allows us to neglect the term $f_3(H/H_i)$ in equation (1). The best fits to experimental data (full curves in figures 1 to 3) were obtained by fixing a value of α_H for each non-superconducting sample and then choosing a value of H_i at each temperature. For samples with superconducting temperature higher than 0.2 K (alloys with $x > 0.25$ and multilayers: see table 1) both $\alpha_H(\frac{1}{2} + \beta)$ and H_i were free parameters at each temperature. β was taken to be independent of the magnetic field which explains, for those samples, the discrepancy between fits and experimental data at low temperature and high fields (figures 2 and 3) while fairly good fits are observed otherwise.

Let us now discuss the data on the physical parameters extracted from the fits. First, α_H is lower than 1 at high silicon concentration and increases as x increases: $\alpha_H = 0.4$,

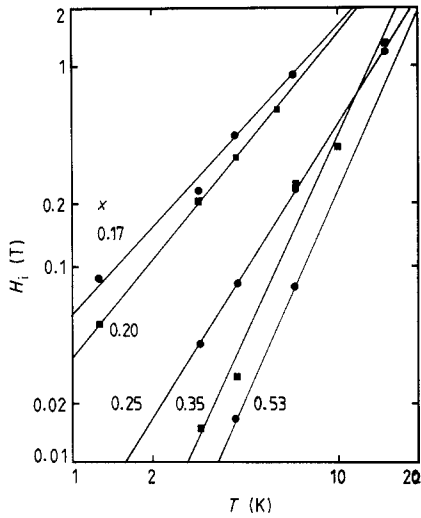


Figure 4. Log-log plot of the parameter H_i deduced from the magnetoresistance data analysis in the case of $\text{Au}_x\text{Si}_{1-x}$ amorphous alloys. x is the gold concentration.

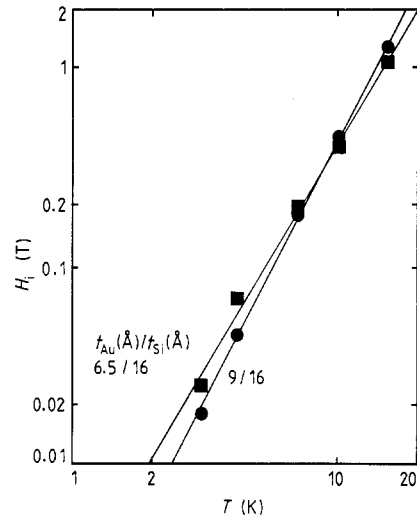


Figure 5. As in figure 4 except for Au/Si multilayers.

0.5, and 0.7 for $x = 0.17, 0.20$ and 0.25 , respectively. For superconducting samples, the value of α_H cannot be unambiguously determined since $\alpha_H(\frac{1}{2} + \beta)$ is a free parameter as a whole. However, assuming $\alpha_H = 1$ leads to values for β larger than those predicted by Larkin (1980) which suggests α_H higher than 1 for those samples. The increase of α_H as the gold concentration increases is unexpected; in contrast to this, larger and larger magnetoresistance is generally observed as metal–insulator transition draws near. For example, in $\text{V}_x\text{Si}_{1-x}$ alloys, $\alpha_H = 1$ and 1.6 for $x = 0.75$ and 0.25 , respectively (Ousset *et al* 1987a, b). The behaviour for $x \leq 0.25$ might be attributed to the decreasing of the spin–orbit scattering rate as the gold concentration decreases: in this concentration range, α_H would be equal to 1 if H_{so} were of the order of 5 to 10 T. Such values for H_{so} do not lead to a maximum as a function of the magnetic field in the magnetoresistance curves in the experimentally covered magnetic field range (less than 6.5 T) so that H_{so} cannot be unambiguously determined for $x \leq 0.25$.

The inelastic scattering rate τ_i^{-1} which is proportional to H_i (see equation (2)) has been determined. For alloys (figure 4) as well as for multilayers (figure 5), $\log_{10} H_i$ varies linearly with $\log_{10} T$ which implies for τ_i^{-1} a temperature dependence of the (classical) form

$$\tau_i^{-1} = aT^P. \quad (5)$$

It must be remarked that equation (5) does not hold in the case of 2D Au/Si multilayers for which the phase breaking rate reaches a constant value τ_s^{-1} as the temperature goes to zero (Cherradi *et al* 1989b). The data of figures 4 and 5 shows that τ_s^{-1} vanishes for 3D samples which confirm that the low temperature behaviour of the phase breaking rate for the 2D multilayers is related to surface effects.

The values of P and (a/D) (cf equation (5)) deduced from figures 4 and 5 are shown on figures 6(a) and 6(b) respectively, as a function of the gold concentration (open

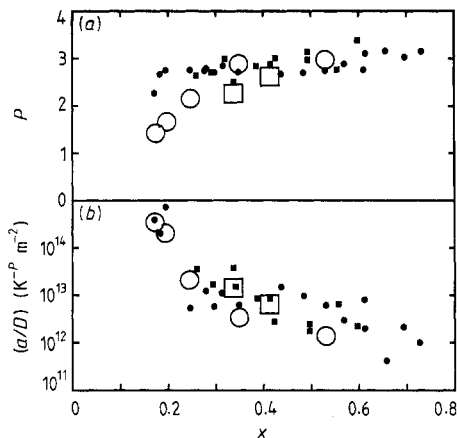


Figure 6. Gold concentration dependence of (a) P and (b) a/D ; see equation (5). Large and small symbols correspond to parameters deduced from the analysis of magnetoresistance and conductivity data, respectively. Squares and circles correspond to parameters deduced from the analysis of multilayer and alloy data, respectively.

symbols). The first remark that can be made is that close values are obtained for alloys and multilayers. Secondly, P increases from 1.4 to 3 as x increases from 0.17 to 0.53. Different theoretical values of P are reported in the literature: Bergmann (1984) and Schmid (1985) respectively found $P = 2$ and $P = 4$ for electron-phonon interaction in the dirty limit, whereas Schmid (1985) obtained $P = 3$ in the clean limit. Generally speaking, experimental data for amorphous alloys lead to values of P between 2 and 4 (Howson and Gallagher 1988) which were attributed to electron-phonon interactions. In particular, Schulte and Fritsche (1986) obtained P values nearly identical to ours as a function of x for $\text{Cu}_x\text{Ti}_{1-x}$ in the composition range $0.41 \leq x \leq 0.63$. For gold concentrations lower than about 0.3 P decreases as x decreases. This behaviour might be attributed to the contribution of electron-electron interactions to the inelastic scattering. For this process, $P = 1.5$ was derived theoretically by Schmid (1973) and by Al'tshuler and Aronov (1979), which is very close to the value $P = 1.4$ obtained for the lowest gold concentration ($x = 0.17$) studied in the present work. It must, however, be noted that the results of the analysis for Si-rich alloys may be influenced by a possible decrease as x decreases of the spin-orbit scattering rate which could not be taken into account as mentioned above.

3.2. Temperature dependence of the conductivity

In this section we examine the respective contributions of electron localisation and interaction on the temperature dependence of the electrical conductivity. The contribution of electron localisation can be written (Fukuyama and Hoshino 1981)

$$\sigma(T) = \sigma(0 \text{ K}) + (e^2/2\pi^2\hbar)(e/\hbar)^{1/2} [3(4H_{\text{so}} + H_i)^{1/2} - H_i^{1/2} - 6H_{\text{so}}^{1/2}]. \quad (6)$$

It is worth noting, as was pointed out by Lindqvist and Rapp (1988), that H_{so} in equation (6) is twice H_{so} in equation (1). In the limit of low temperature and strong spin-

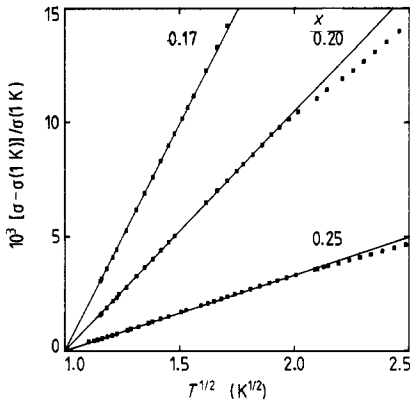


Figure 7. $T^{1/2}$ dependence of the conductivity of non-superconducting Au–Si alloys.

orbit coupling, keeping in mind the temperature dependence of the inelastic scattering rate given by equation (5), equation (6) reduces to

$$\sigma(T) = \sigma(0 \text{ K}) - (e^2/4\pi^2\hbar)(a/D)^{1/2}T^{P/2}. \tag{7}$$

On the other hand, at temperatures high enough for H_{so} to be neglected, equation (6) can be written

$$\sigma(T) = \sigma(0 \text{ K}) + (e^2/2\pi^2\hbar)(a/D)^{1/2}T^{P/2}. \tag{8}$$

The contribution of electron–electron interactions is given by (Lee and Ramakrishnan 1985)

$$\sigma(T) = \sigma(0 \text{ K}) + (1.3e^2/2\pi^2\hbar)(\frac{4}{3} - \frac{3}{2}F_\sigma)^{1/2}(kT/2D\hbar)^{1/2}. \tag{9}$$

As P is larger than 1 (cf figure 6(a)) electron–electron interaction is expected to be predominant at low temperature. Indeed, a $T^{1/2}$ conductivity variation is observed on figure 7 at temperatures lower than about 4 K for non-superconducting alloys as reported for many other amorphous alloys (Howson and Gallagher 1988). Same behaviour has also been observed for a non-superconducting three-dimensional multilayer Au 5 Å/Si 15 Å (Cherradi *et al* 1989b). Assuming, as a first approximation, that the main effect of a magnetic field is to remove the contribution of both electron localisation and superconductivity, more extensive data on electron–electron interaction could be obtained from the temperature dependence of the conductivity in a magnetic field. Two examples are shown on figures 8 and 9 for an amorphous alloy and a multilayer, respectively. The diffusion constant D can then be determined from the $T^{1/2}$ conductivity variation in magnetic field according to equation (9) and compared to its value as calculated from a free-electron model. Except at low gold concentration ($x \leq 0.2$) a large discrepancy was observed between experimental data and free-electron model predictions. An explanation can be derived from magnetoresistance data: figures 4 and 5 show that as soon as the gold concentration goes beyond $x = 0.25$, inelastic mean free paths ($\lambda_i = (\hbar/4eH_i)^{1/2}$, see equation (2)) as large as about 1000 Å may be observed at low temperature which indicates that electron transport may not be purely 3D in the low temperature range. In that case, the temperature dependence of the conductivity should be enhanced which leads, as observed, to an underestimation of the diffusion constant.

At temperatures higher than about 4 K, the conductivity of non-superconducting samples exhibits no more the $T^{1/2}$ behaviour due to electron–electron interaction. This

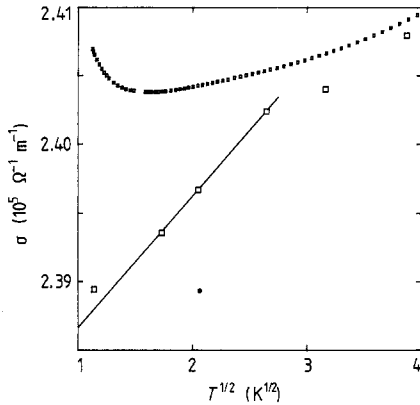


Figure 8. Temperature dependence of the conductivity of the superconducting amorphous alloy $\text{Au}_{0.35}\text{Si}_{0.65}$. Small and large symbols correspond to data obtained in zero and 6 T magnetic field, respectively.

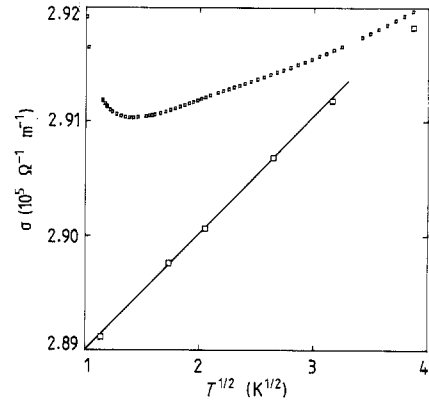


Figure 9. As in figure 8 except for the multilayer $\text{Au}(9 \text{ \AA})/\text{Si}(16 \text{ \AA})$.

is caused by the growing influence of the electron localisation as the temperature increases. At a temperature high enough for the spin-orbit scattering rate to be negligible when compared to the inelastic scattering rate, equation (8) becomes valid and can be rewritten

$$d\sigma/d(\ln T) = (P/2)[\sigma(T) - \sigma(0 \text{ K})]. \quad (10)$$

Equation (10) (and consequently equation (8)) was found to hold as well for alloys as for multilayers in the temperature range roughly from 10–100 K: an example is given on figure 10 for the alloy $\text{Au}_{0.73}\text{Si}_{0.27}$. Such plots allow the determination of the quantities P (figure 10(a)) and a/D (figure 10(b)) which are respectively plotted in figures 6(a) and 6(b) as functions of x (full symbols) together with those deduced from magnetoresistance data. For $x < 0.3$, P values derived from conductivity data are higher than those derived from magnetoresistance data. This is certainly due to the overestimation of the spin-orbit scattering rate in the analysis of the magnetoresistance data of Si-rich alloys, as already mentioned. In contrast to this, for $x > 0.3$, an excellent agreement can be observed on one hand between magnetoresistance and conductivity data and, on the other hand, between alloy and multilayer data.

The conductivity data may also tentatively be fitted in the intermediate temperature range ($T \leq 15 \text{ K}$) according to equations (6) and (9) for non-superconducting or low-temperature superconducting samples. To achieve this purpose $H_i(T)$ (equation (5)) was taken from magnetoresistance data, the free parameters being $\sigma(0 \text{ K})$, H_{s0} and D . A good agreement between theory and experimental data can be observed in figure 11 where full curves are best fits to experimental data obtained from non-linear regressions. The values of D deduced were found to be in good agreement with those obtained from the temperature dependence of the electrical conductivity in a magnetic field. However, the values deduced for H_{s0} strongly depended on the temperature range in which the experimental data was fitted so that reliable values for H_{s0} could not be derived from the fits.

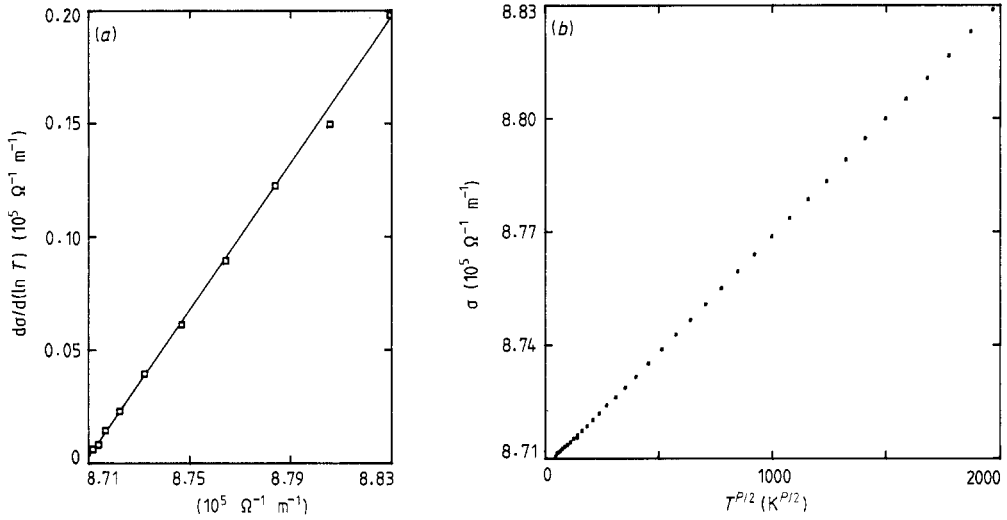


Figure 10. Contribution of the electron localisation to the temperature dependence of the conductivity according to (a) equation (10) and (b) equation (8) in the case of $\text{Au}_{0.73}\text{Si}_{0.27}$ amorphous alloy. The exponent P deduced from the straight line in figure (a) is equal to 3.14.

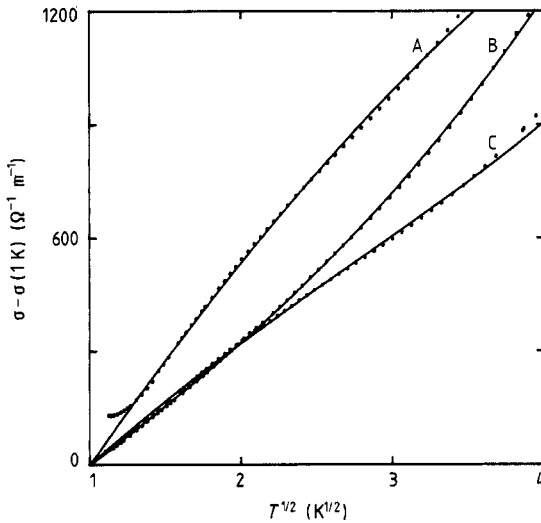


Figure 11. Temperature dependence of the conductivity of $\text{Au}(6.5 \text{ \AA})/\text{Si}(16 \text{ \AA})$ multilayer (curve A), $\text{Au}_{0.17}\text{Si}_{0.83}$ amorphous alloy (curve B) and $\text{Au}_{0.25}\text{Si}_{0.75}$ amorphous alloy (curve C). Full curves are best fits to equations (6) and (9).

4. Conclusion

We have studied the temperature and magnetic field dependence of the conductivity of amorphous alloys $\text{Au}_x\text{Si}_{1-x}$ ($0.17 \leq x \leq 0.73$) and Au/Si multilayers with individual layer thickness t_{Si} from 14 Å to 16 Å and t_{Au} from 5 Å to 16 Å. In this thickness range, both Si and Au layers are amorphous. The experimental data are correctly accounted for by 3D electron localisation and interaction models as well in the case of alloys as in the case of multilayers. Consistent results are derived from the analysis of magnetoresistance

and conductivity data which show that quantum effects are operative in 3D heterogeneous systems and in quantitative agreement with the theory. Alloys and multilayers exhibit closely similar behaviour as a function of the temperature. In particular, the absolute values of the inelastic scattering rate and its temperature dependence are the same in both cases. This result suggests that electron transport properties are insensitive to structural heterogeneities as soon as the length scales of the latter become sufficiently small compared with the characteristic length involved in the electron transport.

References

- Abeles B, Ping Sheng, Coutts M D and Arie Y 1975 *Adv. Phys.* **24** 407
 Al'tshuler B L and Aronov A G 1979 *JETP Lett.* **30** 482
 Al'tshuler B L, Aronov A G, Larkin A I and Khmel'nitzkii D E 1981 *Sov. Phys.-JETP* **54** 411
 Audier M, Guyot P, Simon J P and Valignat N 1985 *J. Physique* **46** C8 443
 Audouard A, Kazoun A, Cherradi N, Marchal G and Gerl M 1989 *Phil. Mag.* **B 59** 207
 Bergmann G 1984 *Phys. Rep.* **107** 1
 Brasen D, Willens R H, Nakahara S and Boone T 1986 *J. Appl. Phys.* **60** 3527
 Carl A, Dumpich G and Hallfarth D 1989 *Phys. Rev.* **B 39** 915
 Cherradi N, Audouard A, Kazoun A and Marchal G 1989a *Solid State Commun.* **70** 315
 Cherradi N, Audouard A, Marchal G, Broto J M and Fert A 1989b *Phys. Rev.* **B 39** 7424
 Dufour C, Brusson A, Georges B, Marchal G, Mangin P, Vettier C, Rhyne J J and Erwin R 1989 *Solid State Commun.* **69** 963
 Fukuyama H and Hoshino K 1981 *J. Phys. Soc. Japan* **50** 2516
 Howson M A and Gallagher B L 1988 *Phys. Rep.* **170** 265
 Kawabata A 1980 *Solid State Commun.* **34** 431
 Larkin A I 1980 *JETP Lett.* **31** 43
 Lee P A and Ramakrishnan T V 1982 *Phys. Rev.* **B 26** 4009
 Lee P A and Ramakrishnan T V 1985 *Rev. Mod. Phys.* **57** 287
 Lindqvist P and Rapp Ö 1988 *J. Phys. F: Met. Phys.* **18** 1979
 Mangin P, Marchal G, Mourey C and Janot C 1980 *Phys. Rev.* **B 21** 3047
 Ousset J C, Askenazy S, Rakoto H and Broto J M 1985 *J. Physique* **46** 2145
 Ousset J C, Rakoto H, Broto J M, Dupuis V, Askenazy S, Durand J, Marchal G and Pavuna D 1987a *Phys. Rev.* **B 35** 5282
 Ousset J C, Rakoto H, Broto J M, Dupuis V, Askenazy S, Durand J and Marchal G 1987b *Phys. Rev.* **B 36** 5432
 Petford-Long A K, Stearns M B, Chang C H, Nutt S R, Stearns D G, Ceglio N M and Hawryluk A M 1987 *J. Appl. Phys.* **61** 1422
 Schmid A 1973 *Z. Phys.* **271** 421
 Schmid A 1985 *Localization, Interaction and Transport Phenomena (Springer Series in Solid State Sciences)* vol 61, p. 212
 Schulte A and Fritsch G 1986 *J. Phys. F: Met. Phys.* **16** L55